Viscosity of a concentrated suspension of rigid monosized particles

H. J. H. Brouwers
Department of Architecture, Building and Planning, Eindhoven University of Technology, P.O. Box 513, 5600 MB Eindhoven, The Netherlands

(Received 1 September 2009; revised manuscript received 11 March 2010; published 10 May 2010)

This paper addresses the relative viscosity of concentrated suspensions loaded with unimodal hard particles. So far, exact equations have only been put forward in the dilute limit, e.g., by Einstein [A. Einstein, Ann. Phys. **19**, 289 (1906) (in German); Ann. Phys. **34**, 591 (1911) (in German)] for spheres. For larger concentrations, a number of phenomenological models for the relative viscosity was presented, which depend on particle concentration only. Here, an original and exact closed form expression is derived based on geometrical considerations that predicts the viscosity of a concentrated suspension of monosized particles. This master curve for the suspension viscosity is governed by the relative viscosity-concentration gradient in the dilute limit (for spheres the Einstein limit) and by random close packing of the unimodal particles in the concentrated limit. The analytical expression of the relative viscosity is thoroughly compared with experiments and simulations reported in the literature, concerning both dilute and concentrated suspensions of spheres, and good agreement is found.

DOI: 10.1103/PhysRevE.81.051402 PACS number(s): 82.70.Kj, 45.70.Cc, 47.55.Kf, 81.05.Rm

I. INTRODUCTION

The rheological behavior of concentrated suspension is of great importance in a wide variety of products and applications, in biology, food, and engineering. There is, therefore, practical as well as fundamental interest in understanding the relationship between the concentration, particle shape, and particle-size distribution on the one hand, and relative viscosity of the suspension (or slurry) on the other.

Here, neutrally buoyant chemically stable (no agglomeration) hard particles in a Newtonian fluid are considered. Furthermore, the viscosity of concentrated slurries is highly sensitive to how this property is measured. Here the effective shear of hard-sphere suspensions at low shear rate and high frequency is addressed, that is to say, the low Reynolds number limit (Stoke's regime). For dilute suspensions, the viscosity-concentration function can be linearized (e.g., the classical hard-sphere result of Einstein [1]). This linearized equation is based on no appreciable interaction between the particles and the coefficient of which depends on particle shape only (and not on size distribution). As loading is increased, this universality is lost, and the viscosity diverges when the associated state of random close packing (RCP) is approached, depending on particle shape and particle size distribution only. One of the most challenging rheological problems has been the development of theoretical and empirical equations for the viscosity of concentrated suspensions. The derivation of a master curve for monosized particle suspensions, in particular the suspensions of spheres, has been the principal goal of many theoretical and experimental studies, and numerous universal equations have been developed in efforts to extend the linear approximations to concentrated suspensions. Such monosized systems are also considered as useful for modeling more complicated polydisperse systems. Here, bimodal particle hard-sphere packing theories are used to derive an analytical expression for the viscosity-concentration function of monosized particles, i.e., the master curve, also called stiffening function.

First, the theories from Farris [2] and Furnas [3] are united. Farris developed and validated a theory to explain the viscosity reduction that follows from mixing discretely sized particles with sufficiently large size ratios. The suspension can then be represented as a coarse fraction suspended in a fluid containing the finer particles, all fractions behaving independently of each other. Furnas addresses in his earliest work the packing fraction of discrete two-component (binary) mixtures, which was later extended to multimodal particle packings. For sufficiently large size ratios, a geometric rule was derived for maximum packing, i.e., the size and quantity of subsequent particle classes have constant ratios. In Sec. II hereof, both theories on particle distribution of noninteracting particles are discussed in detail, and it is shown that the resulting distributions are complimentary. The composition at minimum viscosity as proposed by Farris appears to correspond to the composition at maximum packing fraction as presented by Furnas.

In Sec. III suspension of bimodal particles with small size ratio, i.e., geometrically interacting particles, are studied, recapitulating the model in [2]. Next, the random close packing of these bimodal particle packings is addressed [4]. Here, the unimodal-bimodal limit is studied to relate packing increase (when size ratio increases) and the associated apparent particle concentration reduction (fluid fraction increase). Combining both models, a general equation in closed form is derived that provides the viscosity of a suspension of monosized particles at all concentrations from the dilute limit to the random close packing limit. This equation is governed by the single-sized packing of the particle shape considered (φ_1) and the dilute limit viscosity-concentration gradient (C_1). For spheres, $\varphi_1 \approx 0.64$ and $C_1 = 2.5$. Both for unimodal and for bimodal (small size ratio) suspensions, in Sec. IV the original expressions for the viscosity is compared thoroughly with current models for dilute systems and with experiments in the full concentration range and found to be in good accordance.

II. MULTIMODAL SUSPENSION AND PARTICLE PACKING OF PARTICLES WITH LARGE SIZE RATIO

In [3] the packing fraction of polydisperse discrete particle-size distributions is modeled, and later in [2] an important article on the viscosity of fluids suspended with multimodal particles was addressed. Both authors provided compositions at maximum packing and minimal viscosity, the theories are addressed in this section, and it is demonstrated both theories are fully compatible.

A. Unimodal suspension

The unimodal relative viscosity-concentration function is expressed as $H(\Phi)$, where H is the stiffening factor, the ratio of viscosity with particles divided by the viscosity of the pure fluid. For a hard particle system, H is a function of the particle volume concentration, Φ, and the particle shape only. For dilute suspensions, the virial expansion of the relative viscosity to second order in Φ is

$$\mu = \frac{\eta_{\text{eff}}}{\eta_f} = H(\Phi) = 1 + C_1\Phi + C_2\Phi^2 + O(\Phi^3). \tag{1}$$

For spheres, dominating viscous effects, and ignoring particle interactions, Einstein computed the first-order virial coefficient C_1, also referred to as "intrinsic viscosity" as 2.5 [1]. For nonspherical particles, C_1 has for instance been computed and measured for ellipsoids and slender rods [5–8]. The second-order coefficient C_2 has among others been determined in [9–16].

For more concentrated suspension, the most known phenomenological descriptions are the transcendental function [17,18]

$$H(\Phi) = e^{C_1\Phi/(1-\Phi/\varphi_1)}, \tag{2}$$

and the power-law function [19–23]

$$H(\Phi) = \left(1 - \frac{\Phi}{(1-c\Phi)}\right)^{-C_1} = \left(\frac{\varphi_1 - \Phi}{\varphi_1 - (1-\varphi_1)\Phi}\right)^{-C_1}, \tag{3}$$

as $c=(1-\varphi_1)/\varphi_1$ [23]. Both equations tend to Eq. (1) for $\Phi \to 0$, and diverge for $\Phi \to \varphi_1$, i.e., the critical volume fraction. For low shear rates and without interparticle forces, divergence takes place for Φ tending to 0.58–0.64 [23–27]. This critical volume fraction lies near the random close packing limit, representing the limiting packing fraction above which flow is no longer possible. For spheres, the random close-packed fraction, φ_1, is about 0.64 [28].

In Fig. 1, Eqs. (2) and (3) are set out for $C_1=2.5$ and $\varphi_1=0.64$, which are the applicable values for hard spheres. For high shear rates some ordering is found, e.g., spherical particles tend to from crystalline clusters and the system seems capable to flow at volume fraction $\Phi > 0.64$ [26], but this does not hold for zero and moderate shear rates, as addressed here. Furthermore, it is worthwhile to note that in [29] it was found that when the fluid is Newtonian, the suspension can be considered as Newtonian as well. The rheological properties of hard-sphere suspensions with a solid volume fraction up to 0.3 and a shear rate up to 100 s^{-1} were measured [29]. In [30] a Newtonian plafond was found for shear rates below 10^{-3} s^{-1} even for a solid volume fraction of 0.635, so close to divergence.

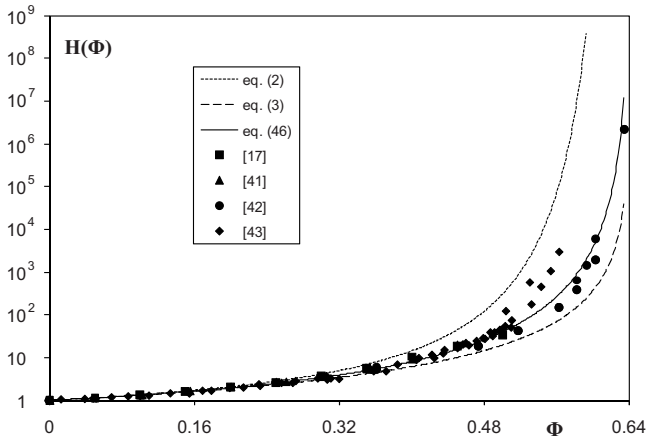

FIG. 1. Stiffening function $H(\Phi)$ as function of particle volume fraction Φ for monosized spheres as predicted by Eqs. (2), (3), and (46) and as measured (taken from Table II and from Fig. 3 [43]).

B. Multimodal suspension

Eveson *et al.* [31] conjectured that a bimodal suspension can be regarded as a system in which the large particles are suspended in a continuous phase formed by the suspension of the smaller particles in the fluid. In [32] this geometric concept was further explored and by carefully executed experiments it could be confirmed. In [2] this concept was used to develop a model based on purely geometric arguments for the viscosity of multimodal suspensions. It was postulated that when large particles are suspended in a suspension of smaller particles, these fractions behave independently. The resulting viscosity can then be expressed in the unique viscosity-concentration behavior of the unimodal suspension. Also the particle size distribution that results in the lowest viscosity, at a given solid concentration, was derived and verified experimentally for spheres [2]. Also for nonspherical particle this concept was successful: for rods and spheres with large size ratio (length more than ten times the sphere diameter) [27,33]. So, to describe the viscosity of multimodal mixes, the unimodal concentration function $H(\Phi)$ is of key importance.

Following the concept of [2], when coarse particles are added to the suspension of fines, the fine particles behave as a fluid toward the coarse. In this case of noninteracting particles, the relative viscosity reads as

$$\mu = \frac{\eta_{\text{eff}}}{\eta_f} = H(\Phi_L)H(\Phi_S), \tag{4}$$

in which Φ_L is the volume fraction of large particles in the total suspension volume and Φ_S is the volume fraction of small particles in small particle plus fluid volume:

$$\Phi_L = \frac{V_L}{V_L + V_S + V_f}, \tag{5}$$

$$\Phi_S = \frac{V_S}{V_S + V_f}. \tag{6}$$

This line of reasoning can be applied to multimodal mixes of n noninteracting particles whereby each fraction is treated independently:

$$\mu = \frac{\eta_{\text{eff}}}{\eta_f} = \prod_{i=1}^{n} H(\Phi_i), \tag{7}$$

whereby size group 1 has the largest particle size and size group n the smallest particle size. The concentration Φ_j of component j is thus governed by

$$\Phi_j = \frac{V_j}{V_f + \sum_{i=j}^{n} V_i}. \tag{8}$$

So the concentration Φ_j is the volume of fraction j divided by the volume fraction of the liquid volume plus the volume of fraction j and the volumes of all smaller fractions (V_{j+1} to V_n). Note that this concentration is not equal to the volume fraction, defined as

$$x_j = \frac{V_j}{V_f + \sum_{i=1}^{n} V_i} = \frac{V_j}{V_T + V_f}. \tag{9}$$

Only for the largest fraction the concentration and volume fraction coincide, so $\Phi_1 = x_1$. The total solid volume fraction is

$$x_T = \sum_{i=1}^{n} x_i, \tag{10}$$

which is not equal to $\Sigma\Phi_j$. The total solid volume fraction in the suspension, x_T, is related to the individual concentrations by

$$1 - x_T = \prod_{i=1}^{n} (1 - \Phi_i). \tag{11}$$

In [2] it was demonstrated that for particles with large size ratio (typically 10 or so), a minimum viscosity is obtained when Φ_j is a constant, i.e., $\Phi_j = 1 - (1 - x_T)^{1/n}$ for $j = 1,2,\ldots, n$, and hence $\mu = H(\Phi_j)^n$.

The volume fraction of fraction j in the entire particle mix of n fractions is defined as

$$c_j = \frac{V_j}{\sum_{i=1}^{n} V_i} = \frac{V_j}{V_T} = \frac{x_j}{x_T}, \tag{12}$$

see Eqs. (9) and (10).

C. Multimodal packing

Furnas [3] studied bimodal random close packings at first instance and extended this to multimodal mixtures. Let φ_1 be the packing fraction of the uniformly sized particles, then by combining two noninteracting size groups, so the small particles are able to fill the void fraction, $1 - \varphi_1$, of the large particles, one obtains as total bimodal packing fraction:

$$\varphi_T(u > u_b) = \varphi_1 + (1 - \varphi_1)\varphi_1. \tag{13}$$

This concept is applicable only when the smaller ones do not affect the packing of the larger size group. Experiments with mixtures of discrete sphere sizes revealed that this is obviously true when $u \to \infty$ [3,34] but that nondisturbance is also closely approximated when the size ratio is about 7–10 (here designated as u_b). Furnas [3] called such mixes "saturated mixtures," in these mixtures the sufficient small particles are added to just fill the void fraction between the large particles. The major consideration is that the holes of the larger particles (characteristic size d_1) are filled with smaller particles (d_2), whose voids in turn are filled with smaller ones (d_3), and so on, until the smallest diameter d_n, whereby the diameter ratio

$$u = d_1/d_2 = d_2/d_3 \quad \text{etc.} > u_b. \tag{14}$$

In general, the packing fraction of multiple mode distributions of n size groups, with $n \geq 1$, then read as

$$\varphi_T(u > u_b) = 1 - (1 - \varphi_1)^n. \tag{15}$$

The volume fraction of each size group j ($j = 1,2,\ldots,n$) in the mixture of n size groups follows as:

$$c_j(u > u_b) = \frac{(1 - \varphi_1)^{j-1} - (1 - \varphi_1)^j}{\varphi_T} = \frac{(1 - \varphi_1)^{j-1}\varphi_1}{1 - (1 - \varphi_1)^n}. \tag{16}$$

It can easily be verified that $\Sigma c_j = 1$. Equation (16) indicates that the quantities of adjacent size groups have a constant ratio

$$\frac{c_j}{c_{j+1}} = \frac{1}{1 - \varphi_1}, \tag{17}$$

as is also the case for the particle size ratio of each subsequent size group (namely u_b), hence a geometric packing is obtained [4].

D. Compositions at minimum viscosity and maximum packing

For fractions with large size ratio (typically 10 or more), Farris derived that minimum viscosity is achieved when all concentrations are equal, whereas Furnas' packing model results in optimum packing when the fractions have a constant ratio [Eq. (11)]. Here, it will be shown that the particle size distribution or composition of the particles is identical.

Following Farris, for minimum viscosity it follows that for the concentration of each size group is the same, Φ_j is constant so that holds

$$\Phi_j = \Phi_1 = x_1, \tag{18}$$

whereby x_1 is the volume fraction of the largest particle size. Combining Eqs. (8), (9), and (18) for size group j yields

$$x_j = x_1\left(1 - \sum_{i=1}^{j-1} x_i\right). \tag{19}$$

Combining this equation with the corresponding equation for size group $j+1$ yields

$$\frac{x_j}{x_{j+1}} = \frac{1}{1-x_1}. \tag{20}$$

So, likewise the composition of the multimodal random close packing recommended by Furnas, also in the recommended composition for minimum viscosity, the quantities of subsequent size groups have a constant ratio; the distribution of the particles is geometric. It was already conjectured in [24] that the composition recommended by Furnas would result in the lowest suspension viscosity.

The total particle volume fraction follows from combining Eqs. (10) and (20) as

$$x_T(u > u_b) = x_1\left(1 + \sum_{i=1}^{n-1} (1-x_1)^i\right) = 1 - (1-x_1)^n. \tag{21}$$

The volume fraction of each size group j $(j=1,2,\ldots,n)$ in the mixture of n size groups follows as:

$$c_j(u > u_b) = \frac{(1-x_1)^{j-1} - (1-x_1)^j}{x_T} = \frac{(1-x_1)^{j-1}x_1}{1-(1-x_1)^n}. \tag{22}$$

Whereas for in the Furnas packing the particles are close packed, in the Farris all particles are suspended in the fluid so that the Furnas packing the most concentrated state. In other words, $x_1 < \varphi_1$ and $x_T < \varphi_T$, φ_1 being the packing fraction associated with random close packing of the monosized packing. Keeping this in mind, one can once more observe the similarity in mix composition by comparing Eqs. (16) and (22).

E. Bimodal particle mixtures

In this section the Furnas and Farris particle compositions are specified in the case of bimodal particles ($n=2$ and $j=1,2$) with large size ratio ($u > u_b$). For bimodal mixes the subscripts "L" and "S" are used instead of "1" and "2", respectively. Following Eqs. (16), Furnas' model provides for optimum bimodal packing

$$c_L = \frac{1}{2-\varphi_1}, \quad c_S = \frac{1-\varphi_1}{2-\varphi_1}, \tag{23}$$

whereby

$$c_L + c_S = 1, \tag{24}$$

indeed. For minimum suspension viscosity, Farris' model yields $\Phi_S = \Phi_L$ or with Eqs. (5) and (6)

$$\frac{V_L}{V_L + V_S + V_f} = \frac{V_S}{V_S + V_f} \tag{25}$$

or using Eq. (9)

$$x_L = \frac{x_S}{1-x_L}. \tag{26}$$

This result also follows from Eq. (20) with $j=1$ applied. For bimodal suspensions in general Eq. (10) yields

$$V_T = V_L + V_S, \quad x_T = x_L + x_S, \tag{27}$$

and for minimum viscosity the fractions of large and small particles in the solid mixture follows from Eq. (12) as

$$c_L = \frac{x_L}{x_L + x_S} = \frac{1}{2-x_L}, \quad c_S = \frac{x_S}{x_L + x_S} = \frac{1-x_L}{2-x_L}, \tag{28}$$

whereby $x_L < \varphi_1$.

From the present analysis one can see that whereas for a unimodal mix the particle volume fraction x_1 (or x_L) is limited to φ_1, for a multimodal mixture the total particle concentration $x_T < \varphi_T$. One can also consider it from the fluid side, for a unimodal mixture the fluid volume fraction, this is $1-x_1$, should be larger than $1-\varphi_1$, which is the void fraction of the random close packing. For multimodal packing, owing to an increased packing fraction, the fluid fraction $1-x_T$ only need to be larger than $1-\varphi_T$. The asymptotic behavior can thus be understood from a particle packing point of view and geometric considerations only. Here, saturated packings were considered, so $u > u_b$, in the following section bimodal packings for which u is close to unity are addressed.

III. BIMODAL MIXTURES WITH SMALL SIZE RATIO

In this section, random bimodal packings and suspensions of bimodal particles with small size ration are analyzed. The geometric model of Farris is known to hold for large size ratios, as outlined in the previous section. Though it seems not to be noticed so far, Farris also extended this model to finite and small size ratios u, which will be addressed here. Furthermore, unimodal random packings on the onset of bimodal packing, so u close to unity, exhibit an increased packing fraction [3,4,34,35]. Here this concept is used to assess the reduction in concentration when u deviates from unity. The combination of this "excess fluid concept" and of Farris' theory finally results in a differential equation for the stiffening function $H(x)$, which is solved analytically.

A. Farris model for small size ratio

The geometric model of Farris is known for large size ratios, which validity has been extensively confirmed (Sec. II). What apparently has not been noticed over the years or at least has not been remarked upon is that in [2] the model is extended to finite and small size ratios. From theory and experiments it was concluded that for interfering particle sizes, Eq. (4) is still applicable but a part f of the smaller fraction should be assigned to the larger fraction, and the remaining part, $1-f$, to the small fraction, hence

$$\Phi_L = \frac{V_L + fV_S}{V_L + V_S + V_f}, \tag{29}$$

$$\Phi_S = \frac{(1-f)V_S}{(1-f)V_S + V_f}, \tag{30}$$

whereby f, the so-called crowding factor, depends on the particle size ratio. For $u=1$ (monosized particles), $f=1$ and in such case μ becomes $H(\Phi)$ as Φ_S becomes 0 [hence $H(\Phi_S)=1$] and Φ_L becomes Φ, see Eq. (4). That is to say, for $u \downarrow 1$, the total particle volume fraction x_T of the unimodal particle suspension reads as

$$x_T = x_L + x_S = \Phi < \varphi_1. \tag{31}$$

On the other hand, $f=0$ for $u^{-1}=0$, i.e., noninteracting sizes as discussed in the previous section. In the latter case, obviously Eqs. (5) and (6) are obtained. For constant x_S and varying x_L [2], provided f as a function of u^{-1}. Obviously, for $u \downarrow 1$, $x_L < \varphi_1 - x_S$ as $\Phi < \varphi_1$. In the vicinity of $u^{-1}=1$, f is approximated by

$$f = 1 - \omega(1-u^{-1}) = 1 - \omega(u-1) + O[(u-1)^2], \tag{32}$$

whereby ω is the derivative of f with respect to u^{-1} at $u=1$. Inserting Eq. (32) into Eqs. (29) and (30) yields the following expressions:

$$\Phi_L = \frac{V_L + V_S}{V_L + V_S + V_f} - \frac{\omega(u-1)V_S}{V_L + V_S + V_f} = \Phi - \omega(u-1)x_S, \tag{33}$$

$$\Phi_S = \frac{\omega(u-1)V_S}{\omega(u-1)V_S + V_f} = \frac{\omega(u-1)x_S}{1-\Phi} + O[(u-1)^2], \tag{34}$$

see Eqs. (9) and (27). Inserting Eqs. (33) and (34) into the stiffening functions appearing in Eq. (4), their Taylor series expansion for $u-1 \to 0$ yields the following expressions for them:

$$H(\Phi_L) = H(\Phi) - \omega(u-1)x_S\left(\left.\frac{dH}{d\Phi}\right|_\Phi\right) + O[(u-1)^2], \tag{35}$$

$$H(\Phi_S) = H(0) + \frac{\omega(u-1)x_S}{1-\Phi}\left(\left.\frac{dH}{d\Phi}\right|_0\right) + O[(u-1)^2] = 1 + \frac{\omega(u-1)x_S C_1}{1-\Phi} + O[(u-1)^2], \tag{36}$$

whereby Eq. (1) has been used in Eq. (36), i.e., the first-order expansion of $H(\Phi)$ in the dilute limit. Substituting Eqs. (35) and (36) in the bimodal stiffening function [Eq. (4)] yields a first-order expression

$$\mu = H(\Phi_L)H(\Phi_S) = H(\Phi) - \omega(u-1)x_S\left(\left.\frac{dH}{d\Phi}\right|_\Phi - \frac{C_1}{1-\Phi}H(\Phi)\right). \tag{37}$$

This equation, based on the concept in [2], expresses the relative viscosity of a monosized suspension a with total concentration Φ that becomes bimodal. The last terms on the right-hand side Eq. (37) govern the stiffening reduction upon the transition of unimodal particles to bimodal particles ($u>1$) in the suspension.

B. Excess fluid for small size ratio

Robinson [36] presented a modification of the Einstein equation by considering the free fluid, i.e., the fluid remaining outside of the suspended particles when they are close packed. Shapiro and Probstein [37] found a correlation between bimodal suspension viscosity and bimodal RCP. Here a model is derived for the case that unimodal particles become bimodal, that is to say, their packing fraction increases and excess fluid is generated. In this model the packing fraction of the suspended particles is relevant.

Equation (13) governs the bimodal packing fraction for saturated packings, i.e., $u>u_b$. In [4] it was demonstrated that for $u-1$ approaching zero, the bimodal packing fraction can be approximated by

$$\varphi_2(u \to 1, c_L) = \varphi_1 + 4\beta\varphi_1(1-\varphi_1)c_S c_L(u-1). \tag{38}$$

Both φ_1 and β depend on the particle shape and the mode of packing (e.g., dense and loose) only, for RCP of spheres, $\varphi_1=0.64$ and $\beta=0.20$ [4]. The parameter β follows from the gradient in packing fraction when a unimodal packing ($u=1$) turns into a bimodal packing ($u>1$), i.e., it is a scaled derivative of φ_2 with respect to u, which is maximum at parity ($c_L=c_S=0.5$).

It follows that along ($u=1$, $0 \le c_L \le 1$), the packing fraction retains it monosized value; physically this implies that particles are replaced by particles of identical size, i.e., maintaining a single-sized mixture, and $x_L+x_S=\varphi_1$. Also along ($u \ge 1$, $c_L=0$) and ($u \ge 1$, $c_L=1$), the packing fraction remains φ_1, as this corresponds to the packing of unimodal small and large particles, respectively.

From Eq. (38) one can see that when a monosized packing becomes bimodal, the packing fraction increases, likewise when particles of large size ratio are combined (previous section). Mangelsdorf and Washington [35] already expressed the increased packing fraction, by combining spheres with small size, in terms of reduced void fraction of the packed bed and created excess volume. In such case, less fluid is needed to fill the voids and excess fluid is created. This means that a packed bed of monosized particles, i.e., $\Phi=\varphi_1$, becomes a suspension when $u>1$. In Fig. 2, this case corresponds to $V_f - V_{\mathrm{rcp}}(1-\varphi_1)=0$ with as volume of the random close packing, $V_{\mathrm{rcp}}=V_T/\varphi_1$: fluid volume V_f in the mixture is just sufficient to fill the voids of the close-packed particles which have a total solids volume V_T.

When $u>1$, the stiffening function diverges when the concentration approaches φ_2 instead of φ_1. Alternatively, one can also say that the packed bed contracts, and the excess fluid becomes available to suspend the particles. This created excess fluid amounts

$$\Delta V_f = \frac{\varphi_2 - \varphi_1}{\varphi_2} V_{\mathrm{rcp}} = \frac{4\beta(1-\varphi_1)c_S c_L(u-1)V_T}{\varphi_1} + O[(u-1)^2], \tag{39}$$

see Eq. (38). The particle volume fraction then reads as

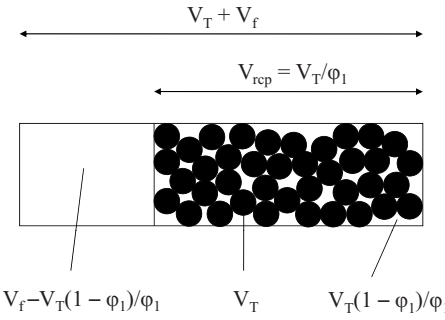

FIG. 2. Schematic representation of a suspension of unimodal particles with total volume V_T and a fluid volume V_f, whereby the particles are arranged in a random close packing (packing fraction φ_1). The volumes of packed bed V_{rcp} and of the free (excess) fluid are indicated.

$$\Phi_2 = \frac{V_T}{V_T + V_f + \Delta V_f} = \varphi_1 - 4\beta\varphi_1(1-\varphi_1)c_S c_L(u-1) + O[(u-1)^2], \tag{40}$$

as $V_T/(V_f+V_T)=\Phi=\varphi_1$ for $u=1$. For a suspension, so when $V_f > V_T(1-\varphi_1)/\varphi_1$ and hence $\Phi<\varphi_1$, see Fig. 2, the reduction in particle volume fraction by letting $u>1$, follows from

$$\Phi_2 = \frac{V_T}{V_T + V_f + \Delta V_f} = \Phi\left[1 - 4\beta\frac{\Phi}{\varphi_1}(1-\varphi_1)c_S c_L(u-1)\right] + O[(u-1)^2], \tag{41}$$

as $V_T/(V_f+V_T)=\Phi$. In other words, Eq. (40) is the special case of Eq. (41) when $\Phi=\varphi_1$, so a monosized random close packing as starting situation. Now, the bimodal stiffening function can expanded for $u\approx 1$:

$$\mu = H(\Phi) - \frac{4\beta(1-\varphi_1)c_S c_L(u-1)\Phi^2}{\varphi_1}\left.\frac{dH}{d\Phi}\right|_{\Phi} + O[(u-1)^2]. \tag{42}$$

In the previous subsection equivalent Eq. (37) was derived, based on the model of Farris for $u\to 1$. Both models and resulting equations will be combined in the next subsection.

C. Stiffening function $H(\Phi)$

The bimodal relative viscosity is governed by both the Farris concept [Eq. (37)] and by the excess fluid volume consideration [Eq. (42)]. Equating both equations, ignoring $(u-1)^2$ and higher terms, and substituting x_S/Φ and x_L/Φ for c_S and c_L, respectively, yields

$$\omega\left(\frac{dH}{d\Phi} - \frac{C_1}{1-\Phi}H(\Phi)\right) = \frac{4\beta(1-\varphi_1)x_L}{\varphi_1}\frac{dH}{d\Phi}, \tag{43}$$

and it can be seen that both $u-1$ and x_S have cancelled out from the first-order terms. This implies that by combining both expansions [Eqs. (37) and (42)], the actual bimodal character of the particle mix, governed by size ratio u and composition x_S (or x_L) is irrelevant.

In the limit of $u\to 1$ and Φ tending to φ_1 (and hence $x_L \to \varphi_1 - x_S$), both $dH/d\Phi$ and $H(\Phi)$ tend to infinity, but $dH/d\Phi$ dominates H and hence $H/(dH/d\Phi)$ tends to zero, i.e., the second term on the left-hand side of Eq. (42) can be ignored. This feature of the stiffening function $H(\Phi)$ is confirmed by Eqs. (2) and (3), and will here be verified *a posteriori* too. This insight implies that

$$\omega = \frac{4\beta(1-\varphi_1)(\varphi_1 - x_S)}{\varphi_1}. \tag{44}$$

In case $x_S=0$ and hence $x_L=\Phi$, $\omega=4\beta(1-\varphi_1)$, and combining Eqs. (43) and (44) now yield as governing differential equation of the monosized system in the entire concentration range

$$\frac{C_1 H(\Phi)}{(1-\Phi)\left(1-\frac{\Phi}{\varphi_1}\right)} = \frac{dH}{d\Phi}. \tag{45}$$

Separation of the variables H and Φ, integration and application of $H(\Phi=0)=1$ yields

$$H(\Phi) = \left(\frac{1-\Phi}{1-\frac{\Phi}{\varphi_1}}\right)^{C_1\varphi_1/(1-\varphi_1)}. \tag{46}$$

This equation is an analytical expression for the unimodal stiffening function and is derived employing theoretical considerations only. It contains two parameters, the first-order virial coefficient C_1 of the considered particle shape ($C_1=2.5$ for spheres, the Einstein result) and the random close packing fraction φ_1 of the considered particle ($\varphi_1 \approx 0.64$ for spheres). Hydrodynamic effects are accounted for by C_1 only, governing the single particle hydrodynamics, and the remaining part of the model is governed by geometric considerations. The stiffening function diverges when the particle concentration Φ approaches φ_1.

The derivation presumed that $H(\Phi)/(dH/d\Phi)\to 0$ for $\Phi\to\varphi_1$. From Eq. (46) it readily follows that this condition is met. It also follows that in the entire concentration range $0\le\varphi<\varphi_1$; $dH/d\varphi > C_1 H(\varphi)/(1-\varphi)$, so that the last two terms on the right-hand side of Eq. (37) imply a viscosity reduction indeed.

IV. RELATION WITH PREVIOUS WORK

In Sec. III an analytical expression for the stiffening function is derived based on expressions for bimodal suspensions with small size ratio. In this section these underlying equations and the ultimate expression are compared with various experimental and computational results reported in literature.

A. Small size ratio: Random close packing

For one case, $x_S=0.25$, in [2] stiffening functions versus x_T for various u^{-1} (Fig. 4 from [2]) were presented and values of the stiffening factor f against the inverse size ratio u^{-1} ranging from zero to unity follow. In Table I these values of f versus u^{-1} are summarized, and they are set out in Fig. 3. From this data, $\omega=0.18$ can be derived [Eq. (32)]. Substituting $\varphi_1=0.58$ and 0.64, $\beta=0.20$ and $x_S=0.25$, the right-hand side of Eq. (44) yields $\omega=0.19$ and $\omega=0.18$, respectively.

TABLE I. Crowding factor f versus inverse size ratio u^{-1} as extracted from Fig. 4 from Farris [2].

u^{-1}	f
1	1
0.477	0.9
0.313	0.75
0.318	0.4
0	0

This comparison indicates that Farris' concept for interacting sizes is valid up to the situation of random close packing and that ω is related to φ_1, β, and x_S indeed, see Eq. (44). It furthermore confirms that Eqs. (35) and (36) both govern the bimodal suspensions viscosity for small size ratio in the entire Φ range.

B. Unimodal: Dilute

For small Φ, Eq. (46) can be asymptotically expanded as Eq. (1) with as first-order virial coefficient C_1, and as second-order coefficient

$$C_2 = \frac{C_1}{2}\left(\frac{(C_1+1)\varphi_1+1}{\varphi_1}\right). \quad (47)$$

For spheres, substituting $C_1=2.5$ and $\varphi_1=0.64$ yields $C_2=6.33$. This value matches very well with $C_2=6.17$ as computed in [10], who extended Einstein's first-order approximation for noninteracting spheres. From this second-order term, 2.5 originates from the far-field hydrodynamics, 2.7 from the near-field hydrodynamics and 0.97 from Brownian stresses. By [11,15,16] compatible values of 5.95, 6.03, and 5.56, respectively, or C_2 were computed. This latter value of [16] is based on Fig. 3 from [16], where most likely k_H is set out (instead of $k_H[\eta]$) and on Eq. (36) from [16], where $k_H[\eta]^2$ is given (instead of $k_H[\eta]$), $[\eta]$ being the apparent viscosity (i.e., the first-order coefficient C_1). Hence $k_H[\eta]^2$ represents the second-order coefficient C_2, expressed in $[\eta]$ and k_H, the Huggins coefficient (named after [9]). With these adjustments and considering $[\eta]=C_1=2.5$ for spheres, the formulas and definitions (e.g., of Huggins coefficient k_H) are in line with the commonly used ones. The monosized value of k_H plotted in Fig. 3 from [16] (i.e., at $X_L=0$ and at $X_L=1$) amounts 0.89 and hence aforementioned $C_2=5.56$ is obtained.

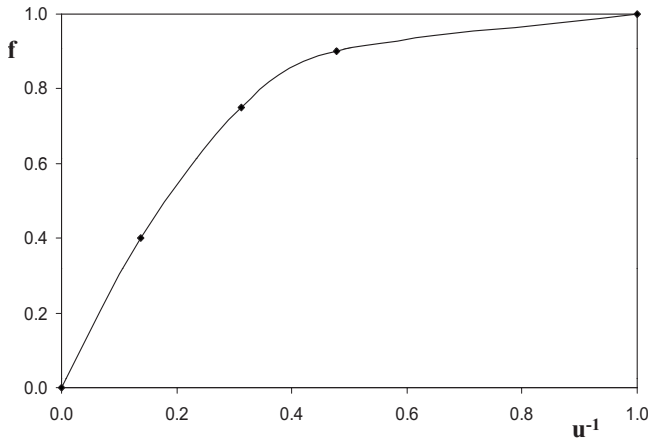

FIG. 3. Values of crowding factor f versus inverse size ratio u^{-1}, taken from Table I. Line is drawn to guide the eye.

The present $C_2=6.33$ is also in line with the second-order expansion of the empirical equations proposed in [38,39], and with the model derived in [40]

$$H(\Phi) = \frac{1}{1-2.5\Phi} = 1 + 2.5\Phi + 6.25\Phi^2 + O(\Phi^3), \quad (48)$$

which turned to be accurate at low and even moderate concentrations ($\Phi \leq 0.3$). For nonspherical particles, C_1 is larger than 2.5 and Eq. (47) can then be approximated by

$$C_2 = \frac{C_1^2}{2}. \quad (49)$$

This expression is compatible with measured and computed second-order coefficients [9,12,13], which typically have denominators ranging from 2 to 2.5, i.e., a Huggins coefficient of 0.4 to 0.5.

C. Small size ratio: Dilute

For bimodal suspensions with small size ratio, Eq. (42) was derived. Substituting in this equation the expansion for dilute suspensions [Eq. (1)] yields

$$\mu = 1 + C_1\Phi + \left(C_2 - \frac{4\beta C_1(1-\varphi_1)c_S c_L(u-1)}{\varphi_1}\right)\Phi^2, \quad (50)$$

whereby C_2, the monosized second-order coefficient of the stiffening function, is given by Eq. (47). One can see that the size effect is having an effect on the second-order term only. The first-order term is applicable to the case whereby the volume occupied by the spheres is negligible and hence does not reckon with sizes. Accordingly, the bimodal particle size distribution does not affect this term (C_1), it is governed by the total solid concentration Φ only. The second-order term, on the other hand, is directly related to the particle size ratio and the composition of the bimodal mix, governed by $u-1$ and $c_S c_L$ [with c_S and c_L coupled by Eq. (24)], respectively. The viscosity reduction is governed by the last term on the right-hand side, containing the reduction in packing fraction by combining two fractions with different particle sizes (bimodal volume contraction), and C_1, the Einstein coefficient, which is also entering the second-order term.

For dilute suspensions of bimodal spheres, the same expression as Eq. (50) was found before [11,16]. In [11] the last term was computed for various size ratio u (u was referred to "λ"), which are used for reference here. As C_2 they determined 5.95, composed of $2.5+(I^H+I^B)$ at $u=1$ (Table 1 from [11]). For $u \neq 1$, a similar parabolic equation as Eq. (50) was obtained to account for the viscosity reduction. The bimodal viscosity reduction, $4\beta C_1(1-\varphi_1)(u-1)/\varphi_1$ appearing in the second term of the second-order term of Eq. (50), corresponds to their $2(I^H+I^B)$ at $u=1$ minus $2(I^H+I^B)$ at $u \neq 1$.

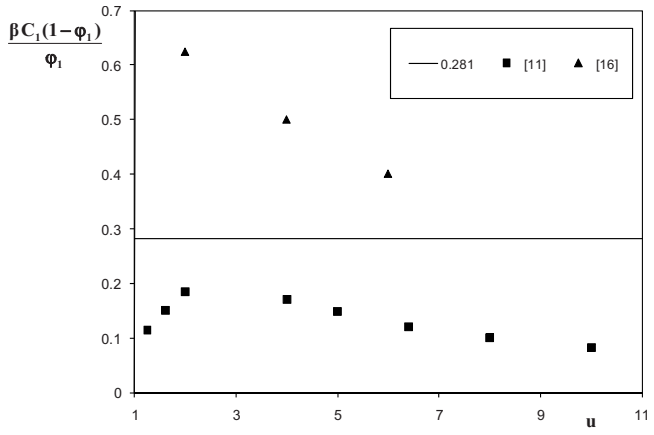

FIG. 4. Bimodal reduction in the second order coefficient as computed by Wagner and Woutersen [11] and Lionberger [16], against the size ratio u and predicted by computing $\beta C_1(1-\varphi_1)/\varphi_1$ using $\beta=0.20$, $\varphi_1=0.64$, and $C_1=2.5$, yielding 0.281.

Using the data from Table 1 of [11], the resulting $((I^H+I^B)_{u=1}-(I^H+I^B)_u)/2(u-1)$ are plotted in Fig. 4. In this figure also corresponding $\beta C_1(1-\varphi_1)/\varphi_1$ with $\beta=0.20$, $\varphi_1=0.64$, and $C_1=2.5$ are included, yielding $\beta C_1(1-\varphi_1)/\varphi_1=0.281$. The substituted values of C_1, φ_1, and β are those pertaining to spheres, they are all well-defined parameters with prescribed, so nonadjustable values that follow from [1,4,28].

Also Lionberger [16] computed the second-order term of the dilute bimodal viscosity. In Fig. 4, $\beta C_1(1-\varphi_1)/\varphi_1$ values that can be extracted from the parabolic curves in Fig. 3 from [16] are included as well, using the corrections explained above.

One can see that the value following the current model (0.28) is located between the predictions of both referred studies and in good agreement. The presented analysis and comparison confirms that the viscosity reduction by mixing two particle sizes can fully be explained indeed by the associated increased packing ability of such bimodal mixes, i.e., by geometric consideration only.

D. Unimodal: Concentrated

Next, the obtained stiffening function is compared with experimental data of unimodal suspensions, from dilute to concentrated (close to divergence). In Fig. 1 measured relative viscosity values are set out, taken from [17,41,42], which are all listed in Table II. Furthermore, in Fig. 1 all data set out in Fig. 3 from [43] are included, originating from [43] and three other references quoted in [43].

In [17,41] glass spheres of a very narrow distribution were used for viscosity measurements. Reference [42] used

TABLE II. Values for the stiffening function $H(\Phi)$ as measured in [17,41,42,44] and computed with Eq. (46) for $\varphi_1=0.61$ and $\varphi_1=0.64$.

Φ	[17]	[41]	[42]	Eq. (46) $\varphi_1=0.61$	Eq. (46) $\varphi_1=0.64$	[44]
0	1	1	1	1	1	1
0.050	1.145			1.143	1.143	
0.100	1.342	1.33		1.334	1.332	
0.102		1.34		1.343	1.341	
0.150	1.621			1.597	1.591	
0.155		1.67		1.629	1.623	
0.200	2.024	2.08		1.976	1.962	
0.250	2.632	2.72		2.553	2.516	
0.261		2.75		2.720	2.676	
0.298		3.60		3.449	3.362	
0.300	3.636	3.68		3.498	3.408	2.97/2.99
0.350	5.556	5.45		5.208	4.971	
0.361			5.4/5.9	5.768	5.472	
0.400	10.53	9.30		8.778	8.076	9.4/9.6
0.450	18.18	20.4		18.09	15.49	18.4/18.6
0.473			18.3	28.08	22.74	
0.500	33.33			53.94	39.41	
0.517			41.6/43.1	90.83	60.09	
0.562			149	822.9	249.5	
0.582			386/644	5640	892.9	
0.593			1436	3.6×10^5	2019	
0.603			1931/5941	1.9×10^6	5236	
0.634			2.2×10^6		11.8×10^6	

monodisperse samples of crosslinked polystyrene microgels dispersed in bromoform were employed, and the zero-shear viscosity determined. These suspensions were found to take the same φ_1 as in macroscopic random close packings (e.g., of glass spheres). From Table II it follows that all three sets of measured relative viscosities closely agree with each other in the entire concentration range. The data taken from [43] concern Poly(methyl methacrylate)-Poly(hydroxy stearic acid) spheres in decalin, decalin-tetralin mixtures, mineral spirits, and SiO_2 spheres in ethylene glycol-glycerol mixtures.

For high sphere loads, $\Phi > 0.4$, Eqs. (2) and (3) overestimate and underestimate, respectively, the measured values. Equation (2) could be better fit to the data by augmenting φ_1, but this also implies that divergence will take place at a packing fraction higher than pertaining to random close packing. In Fig. 1, Eq. (46) is set out from $\Phi=0$ to Φ approaching φ_1, with $\varphi_1=0.64$. One can see that in the full concentration range, Eq. (46) and experiments are lying close together. It appears that the algebraic divergence with exponent $C_1\varphi_1/(1-\varphi_1)$, for the considered spheres with $\varphi_1=0.64$ and $C_1=2.5$ taking a value of 4.4, matches the empirical data well. In Table II the computed values are included, as well those computed with Eq. (46) using $\varphi_1=0.61$. For the glass sphere experiments and moderate Φ sphere loads, one can see that Eq. (46) with $\varphi_1=0.61$ yields better agreement. This limiting value of Φ was observed in [25,26].

E. Small size ratio: Concentrated

For bimodal suspensions with small size ratio, Eq. (42) was derived. Using Eq. (46) to substitute H and $dH/d\Phi$ in Eq. (42) yields

$$\mu = \left(\frac{1-\Phi}{1-\frac{\Phi}{\varphi_1}}\right)^{C_1\varphi_1/(1-\varphi_1)} \left(1 - \frac{4\beta C_1(1-\varphi_1)c_S c_L(u-1)\Phi^2}{(1-\Phi)(\varphi_1-\Phi)}\right). \tag{51}$$

Equation (51) is applicable in the entire concentration range, for $\Phi \to 0$, Eqs. (46) and (51) tend to Eqs. (1) and (50), respectively.

The relative viscosity of concentrated bimodal suspensions of glass spheres with small size ratio ($u=2.33$) was measured in [44], with total concentrations Φ amounting 0.30, 0.40, and 0.45. In Table II their experimental monosized values are included. One can see that their values are in line with those of [17,41] and that also for them Eq. (46) with $\varphi_1=0.61$ provides best agreement with their monosized values.

For the highest concentration, $\Phi=0.45$, the values of [44] are set out in Fig. 5. In this figure, also Eq. (51) with $\beta=0.20$, $\varphi_1=0.61$ and $C_1=2.5$ is drawn. In the entire compositional range there is good agreement between Eq. (51) and the experimental values provided in [44].

V. CONCLUSIONS

In the present paper the relative viscosity of concentrated suspensions of monosized and multimodal rigid particles, consisting of equally shaped particles, at zero shear rate is addressed. In the dilute limit, the hydrodynamics of the individual particle prevails, governed by the first-order coefficient C_1 [Eq. (1)], which takes the well-known Einstein value of 2.5 for spheres. When particle interactions cannot be ignored anymore, it is known that for particles with large size ratios, the viscosity increase can be described by considering geometric considerations only.

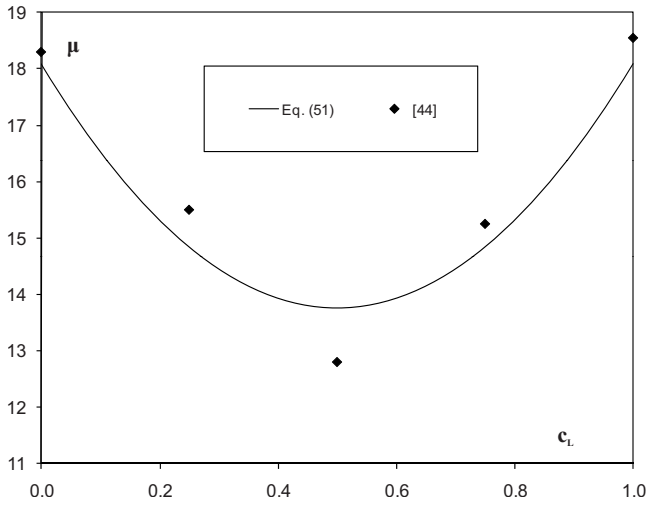

FIG. 5. Bimodal relative viscosity as measured by Krishnan and Leighton Jr. [44] for $\Phi=0.45$ and $u=2.33$ as a function of the large size volume fraction (c_L) and as computed with Eq. (51) using $\beta=0.20$, $\varphi_1=0.61$, and $C_1=2.5$.

It was already observed by [32] and later refined by in [2] that by combining particles which large size ratios, each large fraction can be considered as suspended in a fluid with the smaller fractions. The composition of the multimodal random close packing of such particles at highest packing fraction was modeled in [3]. Here, for these multimodal discretely sized noninteracting particles (size ratio u typically 10 or more), it shown that the composition at lowest relative viscosity ([2]) actually coincides with the composition of a random close packing at highest packing fraction ([3]). These particle arrangements are geometric: i.e., the ratios of particle sizes and the ratios of pertaining quantities are constants.

Next, to obtain an exact equation for the monosized particle viscosity-concentration relation, i.e., the stiffening function; $H(\Phi)$, two approaches are followed. Basically, both are related to packing considerations of bimodal suspensions and packings of discretely sized particles with small size ratio u.

Using the random close packing fraction of such bimodal packings, which contract upon combining two sizes, a differential equation for the apparent fluid increase [Eq. (41)] and associated viscosity reduction is derived [Eq. (42)]. It turns out that the viscosity of these discrete bimodal particle suspensions is governed by the size ratio u, the gradient of the monosized stiffening function for the concentration considered (the Einstein coefficient C_1 for a dilute system), φ_1 and β. The latter two parameters follow from the random close packing of the considered particle shape, φ_1 is the monosized packing fraction and β the packing fraction gradient when a unimodal packing turns into a bimodal packing. In [4] the

parameter β has been derived and values listed and used to model the packing fraction of random continuous power-law packings. Here, it turns out that the bimodal random close packing and related parameter β can be employed to quantify viscosity reduction.

The second line of reasoning follows the observation in [2] concerning the viscosity reduction by combining particles of different size ratios, so not large size ratios only. Farris also considered the case of interacting sizes and found that all bimodal suspensions can be described using the same geometric concept, whereby a crowding factor f (the part of the finer fraction that behaves as large fraction) depends on size ratio u only. Here, this concept is employed to derive a second differential equation [Eq. (37)] that describes the viscosity of a monosized suspension at the onset of turning into a bimodal suspension. This expression contains the gradient of f versus u at $u=1$, viz. ω, governing the gradient when a unimodal suspension becomes a bimodal suspension. So, whereas Eveson [32] and Farris [2] demonstrated the applicability of geometric considerations to bimodal suspensions with large size ratio, here it follows it is also applicable to such suspensions with small size ratio and that it can be used to derive the unimodal stiffening function.

Both approaches yield two differential equations for the bimodal suspension viscosity for small $u-1$. By combining both equations that govern the monosized relative viscosity (stiffening function) at the onset of bimodal suspensions, a governing differential equation [Eq. (45)] for the stiffening function $H(\Phi)$ is derived, and solved in closed form [Eq. (46)]. The resulting analytical expression for the master curve is solely governed by C_1 and φ_1. The resulting stiffening function is found to be in good quantitative agreement with classical hard-sphere experiments [17,41,42]. It appears that the algebraic divergence with exponent $C_1\varphi_1/(1-\varphi_1)$, for the considered spheres with $\varphi_1=0.64$ and $C_1=2.5$ taking a value of 4.4, matches the empirical data well.

Finally, underlying Eqs. (42) and (44) are also validated. By applying Eq. (42) to data concerning the relative viscosity of bimodal suspensions with small size ratio, this expression is found to be in excellent agreement with numerical simulations and experiments (Figs. 4 and 5). Using data provided by [2], Eq. (44) is confirmed as well, which relates ω with φ_1 and β.

ACKNOWLEDGMENT

The author acknowledges the assistance of G. Hüsken with the extraction of the empirical data published in [43] and which have been included in Fig. 1.

[1] A. Einstein, Ann. Phys. **19**, 289 (1906); (in German) **34**, 591 (1911) (in German).
[2] R. J. Farris, Trans. Soc. Rheol. **12**, 281 (1968).
[3] C. C. Furnas, Bureau of Mines Report of Investigation Serial No. 2894, 1928; Bulletin of US Bureau of Mines **307**, 74 (1929); Ind. Eng. Chem. **23**, 1052 (1931).
[4] H. J. H. Brouwers, Phys. Rev. E **74**, 031309 (2006); **74**, 069901(E) (2006).
[5] G. B. Jeffery, Proc. R. Soc. London, Ser. A **102**, 161 (1922).
[6] L. Onsager, Phys. Rev. **40**, 1028 (1932).
[7] W. Kuhn and H. Kuhn, Helv. Chim. Acta **28**, 7 (1945) (in German).
[8] D. H. Berry and W. B. Russel, J. Fluid Mech. **180**, 475 (1987).
[9] M. L. Huggins, J. Am. Chem. Soc. **64**, 2716 (1942).
[10] G. K. Batchelor, J. Fluid Mech. **83**, 97 (1977).
[11] N. J. Wagner and A. T. J. M. Woutersen, J. Fluid Mech. **278**, 267 (1994).
[12] E. S. Boek, P. V. Coveney, H. N. W. Lekkerkerker, and P. van der Schoot, Phys. Rev. E **55**, 3124 (1997).
[13] A. M. Wierenga and A. P. Philipse, Colloids Surf., A. **137**, 355 (1998).
[14] F. M. Van der Kooij, E. S. Boek, and A. P. Philipse, J. Colloid Interface Sci. **235**, 344 (2001).
[15] R. Verberg, I. M. de Schepper, and E. G. D. Cohen, Phys. Rev. E **55**, 3143 (1997).
[16] R. A. Lionberger, Phys. Rev. E **65**, 061408 (2002).
[17] V. Vand, J. Phys. Colloid Chem. **52**, 277 (1948); **52**, 300 (1948).
[18] M. Mooney, J. Colloid Sci. **6**, 162 (1951).
[19] H. Eilers, Kolloid-Z. **97**, 313 (1941) ; (in German) **102**, 154 (1943) (in German).
[20] S. H. Maron and P. E. Pierce, J. Colloid Sci. **11**, 80 (1956).
[21] I. M. Krieger and T. J. Dougherty, Trans. Soc. Rheol. **3**, 137 (1959).
[22] D. Quemada, Rheol. Acta **16**, 82 (1977).
[23] C. I. Mendoza and I. Santamaria-Holek, J. Chem. Phys. **130**, 044904 (2009).
[24] D. I. Lee, J. Paint Technol. **42**, 579 (1970).
[25] J. S. Chong, E. B. Christiansen, and A. D. Baer, J. Appl. Polym. Sci. **15**, 2007 (1971).
[26] J. C. Van der Werff and C. G. de Kruif, J. Rheol. **33**, 421 (1989).
[27] I. Marti, O. Höfler, P. Fischer, and E. J. Windhab, Rheol. Acta **44**, 502 (2005).
[28] G. D. Scott, Nature (London) **188**, 908 (1960); G. D. Scott and D. M. Kilgour, Br. J. Appl. Phys. **2**, 863 (1969).
[29] D. Chan and R. L. Powell, J. Non-Newtonian Fluid Mech. **15**, 165 (1984).
[30] D. A. R. Jones, B. Leary, and D. V. Boger, J. Colloid Interface Sci. **147**, 479 (1991).
[31] G. F. Eveson, S. G. Ward, and R. L. Whitmore, Discuss. Faraday Soc. **11**, 11 (1951).
[32] G. F. Eveson, in *Rheology of Disperse Systems*, edited by C. C. Mill (Pergamon, London, 1959), pp. 61–83.
[33] R. Mor, M. Gottlieb, A. Graham, and L. Mondy, Chem. Eng. Commun. **148–150**, 421 (1996).
[34] R. K. McGeary, J. Am. Ceram. Soc. **44**, 513 (1961).
[35] P. C. Mangelsdorf and E. L. Washington, Nature (London) **187**, 930 (1960).
[36] J. V. Robinson, J. Phys. Chem. **53**, 1042 (1949).

[37] A. P. Shapiro and R. F. Probstein, Phys. Rev. Lett. **68**, 1422 (1992).
[38] W. R. Heß, Kolloid-Z. **27**, 1 (1920) (in German).
[39] T. F. Ford, J. Phys. Colloid Chem. **64**, 1168 (1960).
[40] T. S. Lundgren, J. Fluid Mech. **51**(02), 273 (1972).
[41] T. B. Lewis and L. E. Nielsen, Trans. Soc. Rheol. **12**, 421 (1968).
[42] B. E. Rodriguez, E. W. Kaler, and M. S. Wolfe, Langmuir **8**, 2382 (1992).
[43] Z. Cheng, J. Zhu, P. M. Chaikin, S. E. Phan, and W. B. Russel, Phys. Rev. E **65**, 041405 (2002).
[44] G. P. Krishnan and D. T. Leighton, Jr., Int. J. Multiphase Flow **21**, 721 (1995).

Erratum: Viscosity of a concentrated suspension of rigid monosized particles [Phys. Rev. E 81, 051402 (2010)]

H. J. H Brouwers

(Received 30 July 2010; published 27 August 2010)

DOI: 10.1103/PhysRevE.82.029903 PACS number(s): 82.70.Kj, 45.70.Cc, 47.55.Kf, 81.05.Rm, 99.10.Cd

In Fig. 5 (see Fig. 1 below) of this paper, Eq. (51) is erroneously computed without coefficient C_1. Computing Eq. (51) correctly, so including this factor yields the curve as depicted below. Equation (51) represents the asymptotic approximation for $(u-1)\downarrow 0$ of the suspension relative viscosity μ concerning bimodal spheres.

An alternative approximation follows by substituting Eq. (41) into Eq. (46), yielding

$$\mu = \left(\frac{1 - \Phi\left(1 - 4\beta\frac{\Phi}{\varphi_1}(1-\varphi_1)c_S c_L(u-1)\right)}{1 - \frac{\Phi}{\varphi_1}\left(1 - 4\beta\frac{\Phi}{\varphi_1}(1-\varphi_1)c_S c_L(u-1)\right)} \right)^{C_1\varphi_1/(1-\varphi_1)}.$$

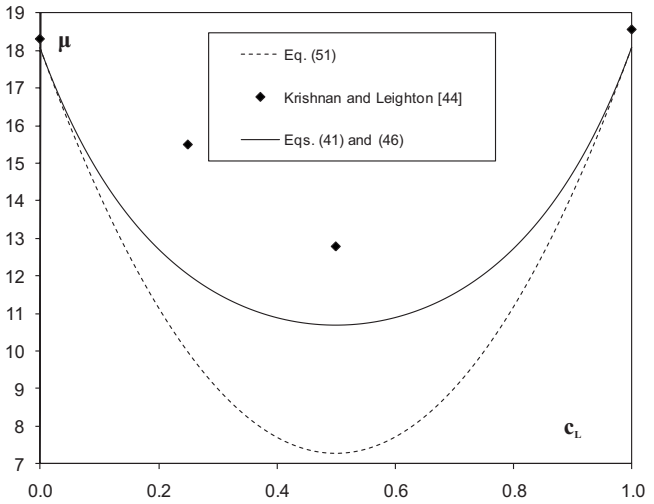

FIG. 1. Bimodal relative viscosity as measured by Krishnan and Leighton Jr. [44] for $\Phi=0.45$ and $u=2.33$ as a function of the large size volume fraction (c_L) and as computed with Eq. (51) and the combination of Eqs. (41) and (46), using using $\beta=0.20$, $\varphi_1=0.61$, and $C_1=2.5$.

Equation (51) is actually the result of asymptotically expanding this equation for small $(u-1)$. In the figure this expression for μ versus c_L is also depicted, again using $C_1=2.5$, $\beta=0.2$, $\varphi_1=0.61$, $u=2.33$, $\Phi=0.45$, and $c_S=1-c_L$. One can see that this approximate expression matches better than Eq. (51) with the empirical data of [44].

The author wishes to thank professor Gary Mavko from Stanford University, California, U.S., for retrieving the error associated with Eq. (51) drawn in Fig. 5.

Erratum: Viscosity of a concentrated suspension of rigid monosized particles [Phys. Rev. E 81, 051402 (2010)]

H. J. H. Brouwers

(Received 24 September 2010; published 29 October 2010)

DOI: 10.1103/PhysRevE.82.049904 PACS number(s): 82.70.Kj, 45.70.Cc, 47.55.Kf, 81.05.Rm, 99.10.Cd

Farris [1] stated that his curves [Fig. 4 of (1)] were based on "constant volume fraction of small spheres." This implies either (i) constant volume fraction of small spheres in the suspension (x_S=const), or (ii) constant volume fraction of small spheres in the bimodal mix (c_S=const). The analysis in our paper is based on case (i). The author shows below that this is incorrect as in fact case (ii) was meant.

Case (i) implies that x_L varies since Φ is a variable and $x_L=\Phi-x_S$ in the limiting condition $(u-1)\downarrow 0$. Case (ii) implies that both c_S and c_L are constant in the bimodal mix ($c_S+c_L=1$), and for the limiting case $(u-1)\downarrow 0$ it means that $x_L=c_L\Phi$ and $x_S=c_S\Phi$. Equation (43), the reasoning following on from this, and applying the limiting value $\Phi\rightarrow\varphi_1$, we obtain

$$\omega = 4\beta(1-\varphi_1)c_L, \tag{1}$$

which implies that now ω is a constant, in contrast to ω based on case (i), expressed by Eq. (44).

Substituting φ_1=0.58 and 0.64, β=0.20 and c_L=0.75 (as c_S=0.25), the right-hand side of Eq. (1) yields ω=0.25 and ω=0.22, respectively. These values are compatible with ω=0.18 which follows from Farris' graph and Eq. (32). It is important to note that the agreement is best for φ_1=0.64, i.e., the value pertaining to the random close packing fraction of monosized spheres.

Following the analysis associated with case (ii), a value of ω is obtained that is constant, as is required, and whose value is compatible with empirical data provided by [1]. Accordingly, Eq. (1) applies instead of Eq. (44); for the rest of the paper this new insight has no additional consequences.

[1] R. J. Farris, Trans. Soc. Rheol. **12**, 281 (1968).

